Sensors and Materials, Vol. 32, No. 8 (2020) 2597–2605
MYU Tokyo

S & M 2286

Fabrication of Needle-type Solid-state CMOS-compatible Glucose Fuel Cell Using Carbon Nanotube for Biomedical Applications

Md. Zahidul Islam,[1,2*] Shigeki Arata,[1] Kenya Hayashi,[1]
Atsuki Kobayashi,[1] and Kiichi Niitsu[1,3**]

[1]Department of Electronics, Graduate School of Engineering, Nagoya University,
Furo-Cho, Chikusa-Ku, Nagoya 464-8603, Japan
[2]Institute of Materials and Systems for Sustainability (IMaSS), Nagoya University,
Furo-Cho, Chikusa-Ku, Nagoya 464-8601, Japan
[3]PRESTO, JST, Kawaguchi, Saitama 332-0012, Japan

(Received June 4, 2019; accepted April 2, 2020)

Keywords: carbon nanotube (CNT), CMOS-compatible, open-circuit voltage (OCV), biomedical application, glucose fuel cell

A solid-state CMOS-compatible glucose fuel cell was fabricated in an anode area using 1D structural carbon nanotubes (CNTs), which exhibits an open-circuit voltage (OCV) of 330 mV and a power density of 7.5 μW/cm^2 at a glucose concentration of 30 mM. The developed fuel cell was manufactured using a semiconductor (CMOS) fabrication process from materials biocompatible with the human body. The CNTs improved the fuel cell performance owing to their high electrocatalytic capability. We have introduced CNTs to the fabrication of a needle-type CMOS-compatible glucose fuel cell. In this paper, we present a (17.5 × 0.7 mm^2) solid-state CMOS-compatible glucose fuel cell with an OCV of 330 mV at a glucose concentration of 30 mM, which is the highest OCV for a glucose fuel cell when the anode area is 4.86 mm^2 (16.2 × 0.3 mm^2). The highest power is 0.36 μW. Power generation is the main challenge in the fabrication of glucose fuel cells for biomedical applications.

1. Introduction

To develop IoT-based healthcare systems, CMOS-compatible glucose fuel cells that offer high-performance functions of low-power computing, sensing, and communications are demanded. To satisfy these demands, CMOS biosensor LSIs are intensively developed.[1–8] CMOS technology improves the energy efficiency of an IoT-based healthcare system. However, energy-autonomous operation using energy harvesting techniques has been difficult. To address this issue, a CMOS-compatible glucose sensor was proposed and developed in 2010.[9] The developed needle-type CMOS-compatible glucose sensor can be fully fabricated using a CMOS-compatible process. The open-circuit voltage (OCV) of a conventional CMOS-compatible glucose fuel cell is only 192 mV, which cannot satisfy the required voltage for the reliable operation of CMOS LSIs. Recently, glucose fuel cells have been considerably developed for use in solid-state CMOS bioelectronic devices owing to the rapid improvements in

*Corresponding author: e-mail: islam.md.zahidul@e.mbox.nagoya-u.ac.jp
**Corresponding author: e-mail: niitsu@nuee.nagoya-u.ac.jp
https://doi.org/10.18494/SAM.2020.2461

their energy efficiency and functioning.[10–18] Solid-state CMOS-compatible glucose fuel cells have been proposed and developed for integration with CMOS circuitries and small systems.[19]

The main components of glucose fuel cells are carbon nanotubes (CNTs) that act as a catalyst of the electrode reactions of glucose and oxygen. CNTs as the catalyst are less specific and exhibit a low reaction rate, but they are stable in long-term applications. Thus, further improvement of the OCV of fuel cells is essential for practical applications.

In this work, a needle-type (17.5 × 0.7 mm^2) solid-state CMOS-compatible glucose fuel cell is fabricated using CNTs for measurements of 0, 10, 20, and 30 mM glucose concentrations. The highest OCV of 330 mV is obtained using 30 mM glucose solution. The performance of the fuel cell is enhanced by CNTs. The enhancement of OCV will lead to the development of implantable devices that could be used for healthcare biomedical applications.

The remainder of the paper is organized as follows. In Sect. 2, the measurement setup of the CMOS-compatible glucose fuel cell is introduced. Section 3 presents the fabrication process and measurement results, and Sect. 4 shows the discussion. Finally, Sect. 5 shows our conclusions.

2. Materials, Methods, and Development

2.1 Materials

The following chemicals and reagents were used in this work: single-walled CNTs purchased from Sigma-Aldrich, 5% Nafion dispersion solution purchased from Wako Pure Chemical Industries, and 2-propanol (IPA), glucose, and other chemicals purchased from Kanto Chemical. All solutions were prepared using Milli-Q water.

2.2 Experimental methods

The developed CMOS-compatible glucose fuel cell is shown in Fig. 1. Its operating principle is based on the energy gained from the complete oxidation of glucose.[20,21] The chemical reactions are as follows:

Anode: $C_6H_{12}O_6 + 6H_2O \rightarrow 6CO_2 + 24H^+ + 24e^-$,

Cathode: $6O_2 + 24H^+ + 24e^- \rightarrow 12H_2O$,

Whole: $C_6H_{12}O_6 + 6O_2 \rightarrow 6CO_2 + 6H_2O$.

Raney platinum cannot mediate the complete oxidization of glucose but mainly mediates the oxidation of glucose to gluconic acid. The main chemical reaction mediated by Raney platinum is as follows:

Anode: $C_6H_{12}O_6 + H_2O \rightarrow C_6H_{12}O_7 + 2H^+ + 2e^-$,

Cathode: $1/2O_2 + 2H^+ + 2e^- \rightarrow H_2O$,

Whole: $C_6H_{12}O_6 + 1/2O_2 \rightarrow C_6H_{12}O_7$.

As shown above, glucose oxidation and oxygen reduction occur on the anode and cathode sides, respectively. To improve the performance of the glucose fuel cell, a glucose solution should be provided. The theoretical electromotive force generated via a partial reaction is 1.30 V.[22]

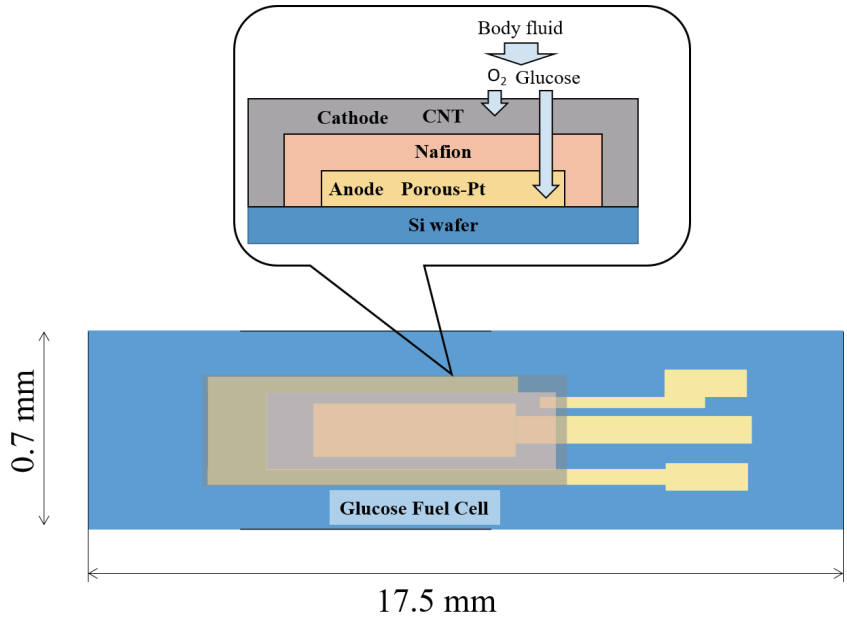

Fig. 1. (Color online) Experimental setup used in this study.

2.3 Experimental development

The process of fabricating the needle-type glucose fuel cell is shown in Fig. 2 and is outlined as follows:

(1) A 6-inch silicon wafer with a 1 μm thermal oxide layer was prepared. The wafer thickness was 625 μm. The fabricated area of each square was 17.5 × 0.7 mm^2. Each cell was arrayed with 0.1 mm left around the cell via the die-cut.

(2) The footprint and anode area were patterned by wet processing. Titanium and platinum of 2 nm and 100 nm thicknesses, respectively, were deposited. Titanium was used as an adhesive layer.

(3) A 100-nm-thick aluminium layer was deposited on the platinum layer in the anode area. It was annealed to form a platinum/aluminium alloy in the anode area. After annealing, the aluminium layer was etched from the platinum/aluminium alloy and only a porous platinum layer remained.[23] The anode area was 4.86 mm^2 (16.2 × 0.3 mm^2).

(4) 0.83% Nafion solution was prepared by 1:5 dilution of Nafion liquid dispersion in IPA [Nafion® perfluorinated resin solution (5 wt%) in a mixture of lower aliphatic alcohols and 45% water (Sigma–Aldrich)]. We spin-coated the Nafion solution at 400 rpm and heated it at 60 and 120 °C for 30 min at each temperature. We repeated the coating and heating processes twice to form a thick Nafion layer, which was then patterned by photolithography. The resist was etched by oxygen ashing using the reactive-ion etching (RIE) technique, resulting in a Nafion layer thickness of 100 nm.

(5) CNTs were dispersed in 0.83% Nafion solution to form a CNT-dispersed solution. We used single-walled CNTs [single-walled ≥95% carbon-based (≥99%), 0.84 nm in average diameter,

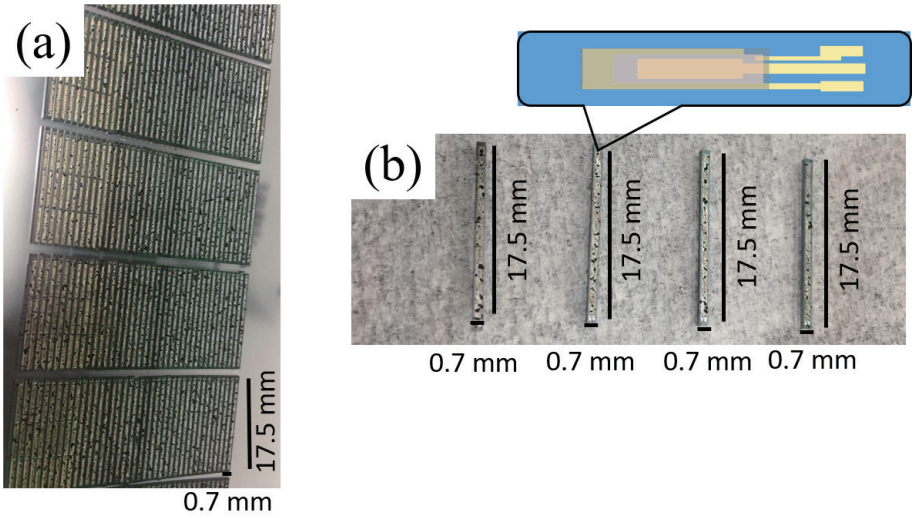

Fig. 2. (Color online) Images of glucose fuel cells fabricated using CNTs: (a) needle-type and (b) separated needle-type fuel cells; 0, 10, 20, and 30 mM glucose solutions are dropped on the anode side.

Sigma–Aldrich]. The CNT solution was spin-coated once and heated. The CNT-coated layer was patterned by photolithography. The resist was etched with oxygen using the RIE technique. The fabricated cells were 17.5 × 0.7 mm^2 in dimension and the wafer was cut into needle chips with a device-side length of 0.1 mm margin on each side.

(6) 0, 10, 20, and 30 mM glucose solutions were dropped on the needle-type fuel cell fabricated using CNTs.

The images in Figs. 2(a) and 2(b) respectively show the completed wafers with the needle-type and separated needle-type fuel cells. Glucose solutions (0, 10, 20, and 30 mM) were dropped on the anode side of the fuel cells, as shown in Fig. 2(b).

3. Experimental Results

The CMOS-compatible glucose fuel cell means that the glucose fuel cell can be integrated into a CMOS. The PMOS (p-type MOS) and NMOS (n-type MOS) fabrication processes were combined and adopted in the CMOS process, which is a standard fabrication process for semiconductor devices because it provides high noise immunity and low power consumption of the devices. Conventional glucose fuel cells use an enzyme, a noble metal, H_2/O_2, methanol/O_2, or microorganisms. This type of fuel cell has low power output and durability. However, CMOS-compatible glucose fuel cells are attractive energy sources of biosensors. CNTs are introduced as a novel tool for fuel cells owing to their inherent properties and conductivity. These glucose fuel cells provide mobile devices for biomedical applications.[24]

In this experiment, the needle-type CMOS-compatible glucose fuel cell had the following structures: porous Pt as the anode and CNTs as the cathode. Figure 3 shows the measured output voltage and current of the prototype with the porous Pt and CNTs, respectively. These structures successfully improved the electrocatalytic capability of the anode and increased the

OCV (19.3, 81.1, 220.0, and 330.0 mV) and current (0.38, 0.55, 1.00, and 1.10 mV) after dropping the glucose solutions (0, 10, 20, and 30 mM). The highest OCV was 330 mV and the peak current was 1.10 μA when using the 30 mM glucose solution. The obtained OCV and current were improved by dropping the glucose solutions on a fuel cell. As a result, a large voltage drop was observed and a portion of the electrode voltage was lost to compensate for the lack of electrocatalytic activity of the CNTs and glucose solutions.

However, the obtained power density decreased from 0.14 to 7.5 μW/cm^2 when the glucose concentration increased as shown in Fig. 4. This is expected to be caused by the insufficient utilization of the catalyst that enhances the effect of activation polarization, as discussed in Ref. 25. The highest OCV was 330 mV and the peak power density was 7.5 μW/cm^2 when the current density was 23.0 μA/cm^2. When the glucose concentration increased, the resistance (50.8 to 300 kΩ) also increased. The highest resistance was 300 kΩ at 30 mM glucose. The potential (330, 220, 81.1, and 19.3 mV) vs current density (23, 21, 11, and 8 μW/cm^2) plot is shown in Fig. 5. The current density of the needle-type glucose fuel cell is higher than that of the conventional glucose fuel cell. Figure 6 shows that the voltage (330, 220, 81.1, and 19.3 mV) depends on the power density (7.5, 4.5, 0.91, and 0.14 μW/cm^2). When the voltage increases, the power density also gradually increases. Nonenzymatic glucose fuel cells exhibit a high power density of 9.459 mW/cm^2, a high current density of 8 mA/cm^2, and an OCV of 0.7128 V at room temperature.[26] The present needle-type (17.5 × 0.7 mm^2) CMOS-compatible glucose fuel cell exhibited an OCV of 330 mV at 30 mM glucose and a power density of 7.5 μW/cm^2. This energy can be applied to mobile devices for biomedical applications.

4. Discussion

Figures 3 and 4 show that the output voltage increases with glucose concentration. Our previous study indicated that both power density and OCV increased with fuel concentration.[19] This performance variation is considerable owing to the insufficient distribution of CNTs used

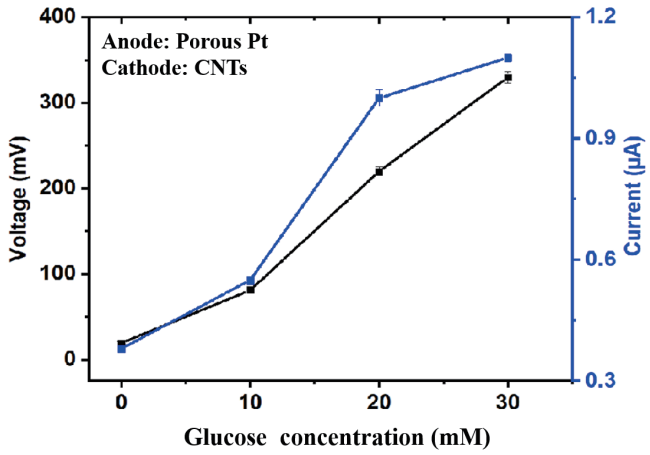

Fig. 3. (Color online) Dependences of output voltage and power on current of fuel cell.

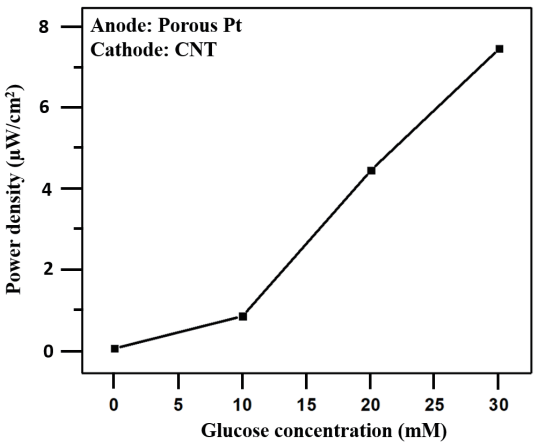

Fig. 4. Power density dependence on glucose concentration.

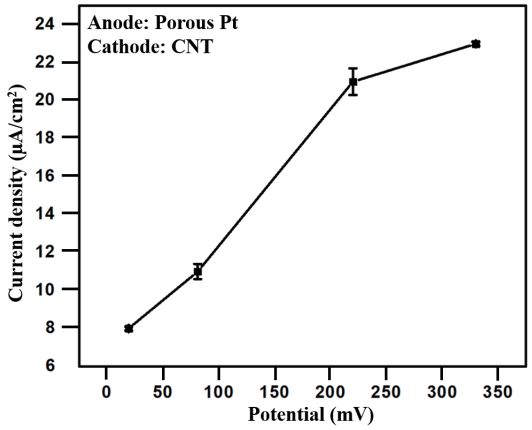

Fig. 5. Potential dependence of current density.

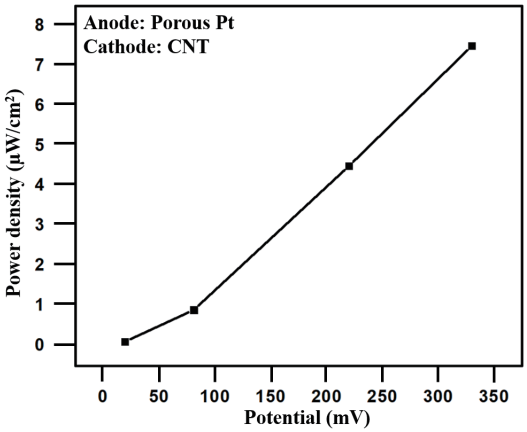

Fig. 6. Potential dependence of power density.

as the cathode. An increased power density results in a low oxygen reduction efficiency or fails to prevent the movement of oxygen to the anode while electrical shortage occurs between the anode and the cathode. The improvement in OCV is discussed from the physical viewpoint. The developed fuel cell shows an improved OCV at 330 mV with 30 mM glucose concentration. From the measurement results, the activation polarization is considered to be related to the energy barrier that must be overcome to initiate a chemical reaction between reactants via a voltage drop in a low-current region.[27]

This higher OCV of 330 mV with a lower output power 0.363 μW is preferable for CMOS circuit design. In CMOS circuit design for power-limited applications, such as biomedical applications, leakage management is important for leakage reduction, power switches, and transistors.[28] A stacked transistor requires a sufficient power supply voltage, which can be obtained by improving the OCV, which in turn makes low-power operation with leakage management feasible. We conclude that this work will contribute to the development of rechargeable devices for biomedical applications.

5. Conclusions

CMOS-compatible glucose fuel cells are attractive energy sources of next-generation healthcare sensors. An OCV of 330 mV is achieved from the needle-type 17.5 × 0.7 mm^2 solid-state CMOS-compatible glucose fuel cell we developed. In this work, glucose solutions (0 to 30 mM) are applied to CNTs to improve the OCV. The CMOS-compatible glucose fuel cells are considered attractive energy sources for next-generation healthcare biomedical applications.

Acknowledgments

This research was financially supported by JST, PRESTO, Grants-in-Aid for Scientific Research (S) (Nos. 20226009 and 25220906), a Grant-in-Aid for Young Scientists (A) (No. 16H06088) from the Ministry of Education, Culture, Sports, Science and Technology of Japan,

the Strategic Information and Communications R&D Promotion Programme (Nos. 121806006 and 152106004) of the Ministry of Internal Affairs and Communications, Japan, TOYOTA RIKEN, and The Nitto Foundation. The fabrication of CMOS chips was supported by Taiwan Semiconductor Manufacturing Co., Ltd. (TSMC, Taiwan), the VLSI Design and Education Center (VDEC), The University of Tokyo in collaboration with Synopsys, Inc., and Cadence Design Systems, Inc.

References

1 K. Niitsu, S. Ota, K. Gamo, H. Kondo, M. Hori, and K. Nakazato: IEEE Trans. Biomed. Circuits Syst. **9** (2015) 607. https://doi.org/10.1109/TBCAS.2015.2479656
2 K. Niitsu, T. Kuno, M. Takihi, and K. Nakazato: IEICE Trans. Electron. E99-C (2016) 663. https://doi.org/10.1587/transele.E99.C.663
3 K. Niitsu, K. Yoshida, and K. Nakazato: Jpn. J. Appl. Phys. **55** (2016) 03DF13. https://doi.org/10.7567/JJAP.55.03DF13
4 S. Tanaka, K. Niitsu, and K. Nakazato: Jpn. J. Appl. Phys. **55** (2016) 03DF10. https://doi.org/10.7567/JJAP.55.03DF10
5 Y. Yamaji, K. Niitsu, and K. Nakazato: Jpn. J. Appl. Phys. **55** (2016) 03DF07. https://doi.org/10.7567/JJAP.55.03DF07
6 H. Ishihara, K. Niitsu, and K. Nakazato: Jpn. J. Appl. Phys. **54** (2015) 04DL05. httsp://doi.org/10.7567/JJAP.54.04DL05
7 T. Kuno, K. Niitsu, and K. Nakazato: Jpn. J. Appl. Phys. **53** (2014) 04EL01. https://doi.org/10.7567/JJAP.53.04EL01
8 K. Niitsu, A. Kobayashi, Y. Ogawa, M. Nishizawa, and K. Nakazato: Proc. IEEE Biomedical Circuits and Systems Conf. (2015) 595.
9 B. I. Rapoport, J. T. Kedzierski, and R. Sarpeshkar: PLOS ONE **7** (2012) e38436. https://doi.org/10.1371/journal.pone.0038436
10 K. Niitsu, M. Sakurai, N. Harigai, T. J. Yamaguchi, and H. Kobayashi: IEEE J. Solid-State Circuits **47** (2012) 2701. https://doi.org/10.1109/JSSC.2012.2211655
11 K. Niitsu, T. Ando, A. Kobayashi, and K. Nakazato: Jpn. J. Appl. Phys. **56** (2017) 01AH04. https://doi.org/10.7567/JJAP.56.01AH04
12 F. Zhang and Y. Lian: IEEE Trans. Biomed. Circuits Syst. **3** (2009) 220. http://citeseerx.ist.psu.edu/viewdoc/download?doi=10.1.1.468.9864&rep=rep1&type=pdf
13 X. Liu, L. Li, and A. J. Mason: IEEE Trans. Biomed. Circuits Syst. **8** (2014) 25. https://doi.org/10.1109/TBCAS.2015.2479656
14 K. Niitsu, A. Kobayashi, Y. Ogawa, M. Nishizawa, and K. Nakazato: Proc. IEEE Biomedical Circuits and Systems Conf. (2015) 595.
15 K. Gamo, K. Niitsu, and K. Nakazato: Proc. IEEE Biomedical Circuits and Systems Conf. (2015) 539. https://doi.org/10.1109/BioCAS.2016.7833746
16 J. Lee, Y. H. Kwak, S. Paek, S. Han, and S. Seo: Sens. Actuators, B **196** (2014) 511. https://doi.org/10.1016/j.snb.2014.02.059
17 H. Lee, A. M. Purdon, and R. M. Westervelt: Appl. Phys. Lett. **85** (2004) 1063. https://doi.org/10.1063/1.1776339
18 K. Niitsu, T. Ando, A. Kobayashi, and K. Nakazato: Jpn. J. Appl. Phys. **56** (2017) 01AH04. https://doi.org/10.7567/JJAP.56.01AH04
19 S. Arata, K. Hayashi, Y. Nishio, A. Kobayashi, K. Nakazato, and K. Niitsu: Jpn. J. Appl. Phys. **57** (2018) 04FM04. https://doi.org/10.7567/JJAP.57.04FM04
20 B. I. Rapoport, J. T. Kedzierski, and R. Sarpeshkar: PLOS ONE **7** (2012) e38436. https://doi.org/10.1371/journal.pone.0038436
21 S. Kerzenmacher, J. Ducrée, R. Zengerle, and F. von Stetten: J. Power Sources **182** (2008) 66. https://doi.org/10.1016/j.jpowsour.2008.03.049
22 S. Kerzenmacher, J. Ducrée, R. Zengerle, and F. von Stetten: J. Power Sources **182** (2008) 1. https://doi.org/10.1016/j.jpowsour.2008.03.031
23 S. Kerzenmacher, U. Kraling, M. Schroeder, R. Bramer, R. Zengerle, and F. von Stetten: J. Power Sources **195** (2010) 6524. https://doi.org/10.1016/j.jpowsour.2010.04.039

24 C. Zhang, J. Hu, X. Wang, X. Zhang, H. Toyoda, M. Nagatsu, and Y. Meng: Carbon **50** (2012) 3731. https://doi.org/10.1016/j.carbon.2012.03.047
25 G. Valdés-Ramírez, Y. Li, J. Kim, W. Jia, A. J. Bandodkar, R. Nuñez-Flores, P. R. Miller, S. Wu, R. Narayan, J. R. Windmiller, R. Polsky, and J. Wang: Electrochem. Commun. **47** (2014) 58. https://doi.org/10.1016/j.elecom.2014.07.014
26 T. Chua and G. Wanga: ECS Meeting Abstract MA **02** (2019) 1453. http://ma.ecsdl.org/content/MA2019-02/33/1453.abstract
27 M. Chu, Y. Zhang, L. Yang, Y. Tan, W. Deng, M. Ma, X. Su, Q. Xie, and S. Yao: Energy Environ. Sci. **6** (2013) 3600. https://doi.org/ 10.1039/C3EE41904E
28 S. Bandyopadhyay, P. P. Mercier, A. C. Lysaght, K. M. Stankovic, and A. P. Chandrakasan: IEEE J. Solid-State Circuits **49** (2014) 2812. https://doi.org/10.1109/JSSC.2014.2350260

About the Authors

Md. Zahidul Islam received his B.S. degree from National University, Gazipur, Bangladesh, in 2007, his M.S. degree from Rajamangala University of Technology Thanyaburi (RMUTT), Thailand, in 2014, and his Ph.D. degree from the Department of Chemical Systems Engineering, Graduate School of Engineering, Nagoya University, Japan. From December 2018 to the present, he has been a researcher at Institute of Materials and Systems for Sustainability (IMaSS), Nagoya University, Japan. His research interests are in electrochemistry, CMOS-compatible glucose fuel cells for biomecical application, solution plasma process, carbon materials, bioengineering, and sensors. (islam.md.zahidul@e.mbox.nagoya-u.ac.jp)

Shigeki Arata received his B.S. degree from Nagoya University, Japan, in 2018 and he is currently pursuing his M.S. degree in the same university. His research interests are in CMOS-compatible fuel cells, bioengineering, and biosensors. (arata.shigeki@b.mbox.nagoya-u.ac.jp)

Kenya Hayashi received his B.S. degree from Nagoya University, Japan, in 2018 and he is presently pursuing his M.S. degree in the same university. His research activity is focused on mixed-signal CMOS integrated circuits for biomedical applications. (hayashi.kenya@b.mbox.nagoya-u.ac.jp)

Atsuki Kobayashi received his B.S. and M.S. degrees in electrical engineering and computer science from Nagoya University, Japan, in 2016 and 2018, respectively, where he is currently working on his Ph.D. degree in electronics. He is currently a research fellow of the Japan Society for the Promotion of Science. His research interest is focused on mixed-signal CMOS integrated circuits for biomedical applications.
(kobayashi.atsuki@d.mbox.nagoya-u.ac.jp)

Kiichi Niitsu received his B.S. degree (summa cum laude), M.S., and Ph.D. degrees in electrical engineering from Keio University, Yokohama, Japan, in 2006, 2008, and 2010, respectively. From 2008 to 2010, he was a research fellow of the Japan Society for the Promotion of Science, a research assistant of the Global Center of Excellence Program, Keio University, and a collaboration researcher of the Keio Advanced Research Center. From 2010 to 2012, he was an assistant professor at Gunma University, Kiryu, Japan. Since 2012, he has been a lecturer at Nagoya University, Nagoya, Japan. Since 2015, he has been a researcher at Precursory Research for Embryonic Science and Technology, Japan Science and Technology Agency. From June 2018 to the present, he is an associate professor in the Graduate School of Engineering, Nagoya University, National University. His current research interests are in the low-power and high-speed technologies of analogue and digital VLSI circuits for biomedical applications. (niitsu@nuee.nagoya-u.ac.jp)